THE JOURNAL OF BIOLOGICAL CHEMISTRY VOL. 283, NO. 10, pp. 6501–6508, March 7, 2008

Structural Dynamics in the Activation of Epac*

Received for publication, September 19, 2007, and in revised form, December 6, 2007 Published, JBC Papers in Press, December 31, 2007, DOI 10.1074/jbc.M707849200

Shannon M. Harper[‡1], Hans Wienk[§1], Rainer W. Wechselberger[§], Johannes L. Bos[‡], Rolf Boelens[§2], and Holger Rehmann[‡3]

From the [‡]Department of Physiological Chemistry and Centre for Biomedical Genetics, University Medical Center Utrecht, 3584 CG Utrecht and [§]NMR Spectroscopy, Bijvoet Center for Biomolecular Research, Utrecht University, 3584 CH Utrecht, The Netherlands

Epac1 is a cAMP-responsive exchange factor for the small G-protein Rap. It consists of a regulatory region containing a cyclic nucleotide binding (CNB) domain and a catalytic region that activates Rap. In the absence of cAMP, access of Rap to the catalytic site is blocked by the regulatory region. We analyzed the conformational states of the CNB domain in the absence and in the presence of cAMP and cAMP analogues by NMR spectroscopy, resulting in the first direct insights into the activation mechanism of Epac. We prove that the CNB domain exists in equilibrium between the inactive and the active conformation, which is shifted by binding of cAMP. cAMP binding results in conformational changes in both the ligand binding pocket and the outer helical segments. We used two different cAMP antagonists that block these successive changes to elucidate the steps of this process. Highlighting the role of dynamics, the superactivator 8-pCPT-2′-O-Me-cAMP induces similar conformational changes as cAMP but causes different internal mobility. The results reveal the critical elements of the CNB domain of Epac required for activation and highlight the role of dynamics in this process.

By transducing biochemical signals from extracellular cues into an intracellular response, biological switches play a crucial role in modulating signaling pathways and functions. One of the oldest stimuli, conserved from bacteria to mammals, is the second messenger cyclic adenosine monophosphate (cAMP) (1). Proteins that respond to cAMP contain a conserved cyclic nucleotide binding (CNB)[4] domain (2). In mammals, CNB domains are found in the regulatory subunit of protein kinase A (PKA), in cyclic nucleotide-responsive ion channels, and in the guanine nucleotide exchange factor (GEF) Epac. Upon cAMP binding, these proteins initiate diverse intracellular signaling events. Epac acts as a GEF for the small G-protein Rap (3, 4). Small G-proteins cycle between a signaling-inactive GDP-bound state and an active GTP-bound state, with the latter exchange activity catalyzed by GEFs such as Epac. Rap itself is involved in cellular processes such as cell adhesion and junction formation (5).

Insight into the mechanism of cAMP activation of CNB domains comes from several crystal structures (6–12). The combined data illustrate that CNB domains utilize a common mechanism to bind and sense cAMP (13). Binding of the ligand induces conserved conformational changes within the domain that are translated in a specific way to activate the protein. This allows the CNB domain to act as a switch unit in such different biochemical processes as kinase activity or guanine nucleotide exchange activity. The core of the CNB domain consists of a β-sandwich that is flanked by the N-terminal helical bundle (NHB) and the C-terminal hinge helix connecting the lid region. The phosphate sugar moiety of cAMP interacts with the so-called phosphate binding cassette (PBC), consisting of two β-strands connected by a short one-turn helix and a loop (14). Binding of cAMP induces tightening of the PBC, repositioning a critical leucine residue. This allows the hinge helix to move closer to the β-sandwich, bringing the lid region in direct contact with the base of the cyclic nucleotide, as well as initiating changes in the NHB. The active conformation is then stabilized by the interaction of the base with the lid (13).

For Epac, the crystal structure of the inactive state of the protein revealed that the CNB domain sterically blocks the access of Rap to the catalytic site in the CDC25 homology domain, which is responsible for mediating the exchange activity (10). The relative orientation between the CNB domain-containing regulatory region and the catalytic region is determined by two contact points, the switch board and the ionic latch. The ionic latch is formed by residues of the NHB and the CDC25 homology domain. The switchboard is localized at the connection between the C terminus of the CNB domain and the catalytic region, where the C-terminal strands of the CNB domain are assumed to form the lid in the ligand-bound conformation. This suggests that in the course of activation, the central β-sandwich moves closer to the hinge and the lid, thereby disrupting the interactions of the ionic latch (10).

As there is little structural information on cAMP-bound Epac, we used NMR spectroscopy to investigate the CNB domain of Epac1. By titrating the cAMP ligand into the isolated domain, we provide insight on the nature of cAMP-induced conformational changes as well as the dynamics of the domain in solution. Using different cyclic nucleotide-based inhibitors, the stepwise mechanism of activation is delineated. Additionally, the role of ligand binding dynamics and the C-ter-

* This work was supported by a long-term fellowship from the Human Frontier Science Program (to S. M. H.), by the Centre for Biomedical Genetics (to H. W. and R. B.), and the Chemical Section of the Netherlands Organization for Scientific Research (to H. R. and J. L. B.). The costs of publication of this article were defrayed in part by the payment of page charges. This article must therefore be hereby marked "*advertisement*" in accordance with 18 U.S.C. Section 1734 solely to indicate this fact.

[1] Both authors contributed equally to this work.

[2] To whom correspondence may be addressed: Utrecht University, Padualaan 8, 3584 CH Utrecht, The Netherlands. Tel.: 31-30-253-4035; Fax: 31-30-253-7623; E-mail: r.boelens@chem.uu.nl.

[3] To whom correspondence may be addressed: UMCU Universiteitsweg 100, 3584 CG Utrecht, The Netherlands. Tel.: 31-88-75-68961; Fax: 31-88-75-68101; E-mail: h.rehmann@UMCutrecht.nl.

[4] The abbreviations used are: CNB, cyclic nucleotide binding; PKA, protein kinase A; NHB, N-terminal helical bundle; PBC, phosphate binding cassette.

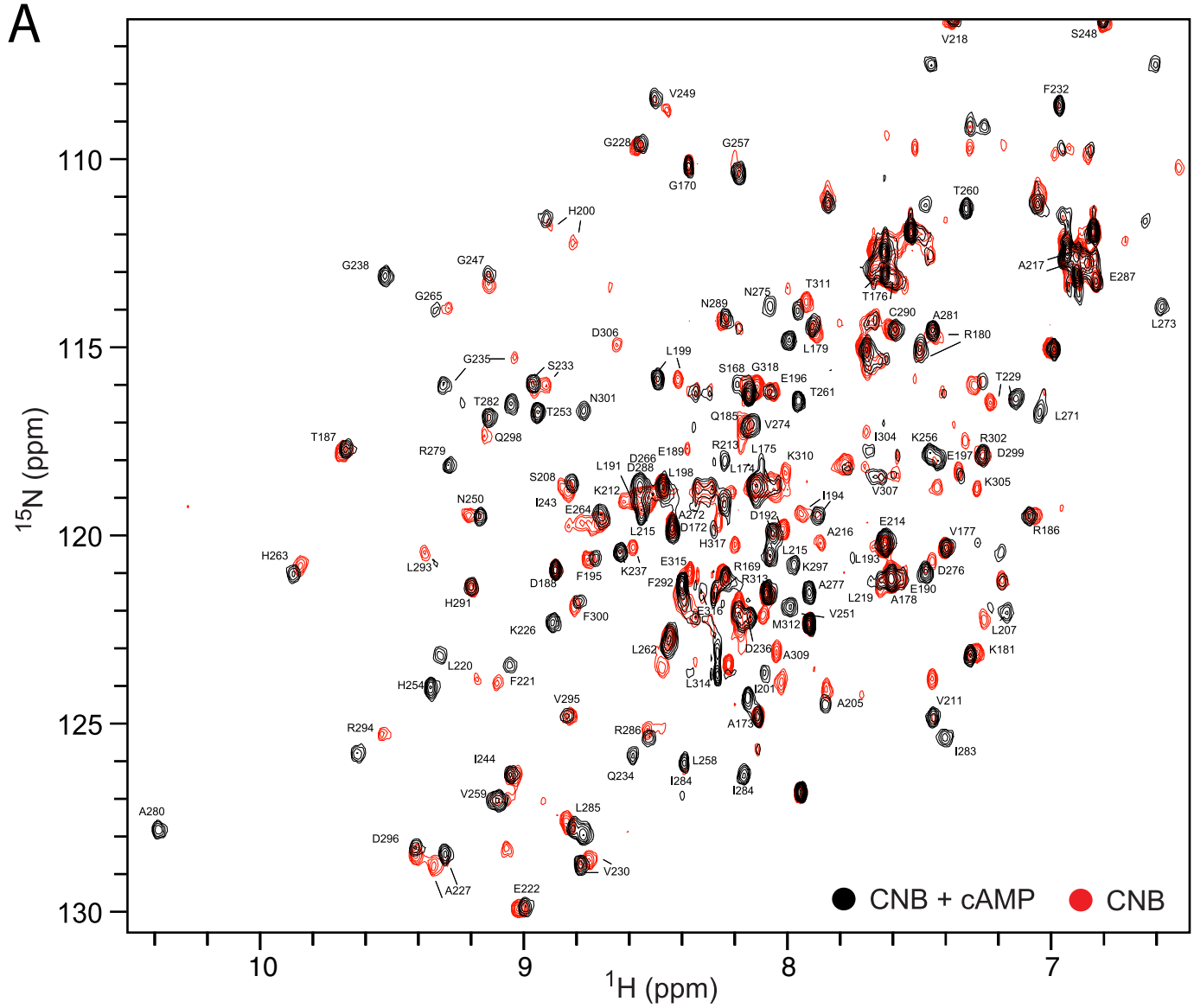

minal hinge region is addressed with the super activator 8-pCPT-2′-O-Me-cAMP.

EXPERIMENTAL PROCEDURES

Expression and Isotope Labeling of the CNB Domain—The CNB domain of Epac1 (residues 169–318) was expressed as a glutathione *S*-transferase fusion protein from the pGEX4T vector (GE Healthcare). BL21 DE3 (Novagen) cells were grown in M9 minimal medium containing 1 g/liter $^{15}NH_4Cl$ (Sigma-Aldrich) as the sole nitrogen source for ^{15}N and 3 g/liter [$^{13}C_6$]glucose as the sole carbon source for $^{15}N/^{13}C$-labeled samples at 37 °C to an A_{600} of 0.6–1.0. Protein production was induced at 20 °C by the addition of 0.5 mM isopropyl-1-thio-β-D-galactopyranoside. After 16 h the cells were harvested, resuspended in 50 mM Tris, pH 7.6, 10% glycerol, 50 mM NaCl, 5 mM EDTA, 5 mM dithiothreitol, and lysed by sonication. The lysate was clarified by centrifugation at 30,000 × *g* for 60 min, and the supernatant was loaded onto a glutathione column (GE Healthcare). The column was washed with 5 column volumes of 50 mM Tris, pH 7.6, 400 mM NaCl, 10% glycerol, 5 mM dithiothreitol and eluted with 50 mM Tris, pH 7.6, 50 mM NaCl, 5% glycerol, 10 mM $CaCl_2$, 5 mM dithiothreitol, and 30 mM glutathione. Glutathione was removed by dialysis, and the glutathione *S*-transferase tag was cleaved by incubation with 40 units of thrombin (Serva) for 3 h at room temperature. The cleaved glutathione *S*-transferase was removed by running the sample over a glutathione column and the buffer then exchanged to 20 mM NaPi, pH 7.0, 5 mM dithiothreitol. Typical yields were 10–30 mg of protein/liter of culture.

NMR Spectroscopy—Experiments were performed at 25 °C in the presence of 10% D_2O. Protein concentration was typically 0.5 mM, unless stated otherwise. ^1H frequencies were calibrated using the internal water signal, ^{15}N and ^{13}C frequencies using indirect referencing (15). Spectra were processed with NMRPipe (16) and analyzed using Sparky. NMR data allowing spectral assignments were acquired using Bruker Avance 600 MHz with cryoprobe, Avance 700 MHz, and Avance 750 MHz NMR spectrometers equipped with 5-mm triple resonance probes. Backbone and side chain assignments of 1 mM cAMP-containing Epac1 CNB domain were established with [^1H,^{13}C]HSQC, [^1H,^{15}N]HSQC, the triple resonance experiments HN(CO)CA, HNCA, (H)CC(CO)NH, CBCA(CO)NH, HNCACB, HNCO, HN(CA)CO, H(CCO)NH, and HBHA(CO)NH, supplemented with H(C)CH-TOCSY, two-dimensional [^1H,^1H]NOESY, (H)CNH-NOESY, H(C)CH-NOESY, and NOESY-[^{15}N]HSQC experiments. For the assignment of ligand-free Epac1 CNB domain the following experiments were used: [^{13}C]HSQC and [^{15}N]HSQC, HNCACB, HNCA, HNCO, (H)CC(CO)NH, HBHA(CO)NH, TOCSY-[^{15}N]HSQC, NOESY-[^{15}N]HSQC, and H(C)CH-TOCSY. All NMR experiments were recorded essentially as described (17). The program TALOS (18) was used to assess the secondary structure elements of the ligand-free and cAMP-bound Epac1 CNB domain. Titration experiments were performed using a Bruker Avance 600 MHz spectrometer with cryoprobe on ^{15}N-labeled Epac1 CNB domain NMR sample by stepwise addition of small aliquots of concentrated cAMP, Rp-cAMPS, N^6-phenyl-cAMP, or 8-pCPT-2′-O-Me-cAMP stock solutions (BioLog). Eight [^1H,^{15}N]HSQC spectra were recorded with increasing ligand concentrations of 0.5, 0.8, 1, 10, 100, 500, and 1000 μM.

Proton-deuterium exchange experiments were performed on a Bruker Avance 600 MHz spectrometer with cryoprobe. ^{15}N-labeled Epac1 CNB domain NMR samples, either in the absence or presence of 1 mM cAMP, were lyophilized and resolved in 500 μl of D_2O. In the course of 24 h, 150 short [^1H,^{15}N]HSQC experiments (~9.75 min each) were recorded. The first spectrum was obtained after a dead time of 15 min. The time dependence of the peak intensity was fitted as single exponential decay using three-parameter curve fitting, followed by a 500-step Monte Carlo simulation by use of the program CurveFit to determine k_{ex}.

RESULTS

Both the unbound and cAMP-bound forms of the CNB domain of Epac1 feature [^1H,^{15}N]HSQC spectra with a well dispersed ^1H dimension, indicative of a folded protein (Fig. 1*A*). Using standard triple resonance methods, the backbone and side chain resonances of the protein were assigned. In the cAMP-free state, 67% of the backbone amide groups were assigned unambiguously and for the cAMP-bound state 85% (Fig. 1*B*). The lower percentage of assignment in the cAMP-free state is caused by both spectral overlap and missing peaks. These missing peaks imply the presence of internal dynamics on a μs-ms time scale in the absence of cAMP. Additionally, in the bound state a series of unambiguous nuclear Overhauser effects were assigned connecting the cAMP molecule with residues Val^{251} and Val^{259} (data not shown), demonstrating that cAMP is indeed bound to the protein.

The secondary structure elements for both the unbound and cAMP-bound forms of Epac1 were determined using the chemical shift analysis program TALOS (18) and are in good agreement with the crystal structure of Epac2, demonstrating that the isolated CNB domain behaves similarly as in the full-length protein (9, 10) (Fig. 1*B*). Overall, the secondary structure elements of the unbound and bound domains are highly similar, confirming that binding of cAMP does not induce global changes in the overall structure of the protein (Fig. 1*B*). However, cAMP binding does result in a shortening of the hinge helix, a clear indication that cAMP causes structural changes in the C-terminal region. Similarly, an induction of a kink in the hinge helix was observed for PKA upon activation (8). This is in contradiction to modeling studies on Epac that suggested a

FIGURE 1. **NMR spectra and secondary structure of Epac1 CNB domain.** *A*, [^{15}N-^1H]HSQC spectra of Epac1 CNB domain in the absence (*red*) and presence (*black*) of cAMP. Assigned peaks are labeled accordingly. *B*, the CNB domain of Epac1 (residues 169–318) used for the NMR study was aligned to CNB domains with known structure (residues numbered according to Epac1): *Channel*, cyclic nucleotide-regulated potassium channel from *Mesorhizobium loti* (Protein Data Bank code 1u12) (12); *PKA*, protein kinase A (Protein Data Bank code 1rgs) (6); *Epac2*, (Protein Data Bank code 2byv) (10). Residues identical to Epac1 are highlighted by *gray background*. The general secondary structure elements are indicated schematically under the alignment. The secondary structure properties of the individual residues as calculated by the program TALOS (18) from the cAMP-free and the cAMP-bound data set are given by *lowercase* letters: *c*, coiled; *h*, α-helical; *s*, β-strand; –, residue unassigned. Residues that adopt a double conformation in the absence of cAMP are printed in *bold*.

cAMP-induced transition of the lid region into a helical structure (19, 20).

Titration of cAMP to Epac1—The structural consequences of cAMP binding were assessed by titrating cAMP into the protein solution and monitoring changes in the [^{15}N,^{1}H]HSQC spectra, where each peak corresponds to a particular amino acid and thus provides a structural readout throughout the domain (Fig. 2*A*). Addition of cAMP produced changes throughout the spectrum, with the majority of peaks displaying slow exchange behavior (for example, residues His^{200} and Gln^{298} in Fig. 2*A*). Additionally, some peaks appeared upon ligand addition, suggesting a slow exchange where the residue in the absence of cAMP is either not detectable under the experimental conditions or located in a remote area of the spectrum (for example, residue Arg^{279} in Fig. 2*A*). For visualization, the observed chemical shift differences were mapped on the ligand-free crystal structure of the CNB domain of Epac2 with cAMP modeled in from the PKA crystal structure (Fig. 2*B*). A multitude of residues clustered around the cAMP molecule are affected. These residues are particularly localized in the PBC, which is in close proximity to the phosphate sugar moiety of cAMP, and in the sheet formed by the β-strands 2, 7, 4, and 5 (β-2-7-4-5-sheet), which is shielding one side of the cAMP molecule. A strong deshielding of residue Arg^{280} in the PBC, expected to be in close proximity to the phosphate moiety, is observed upon cAMP binding (Fig. 1*A*). These changes predominately reflect changes in the electronic environment induced by the presence of the cAMP molecule. It is interesting to note changes in regions more distant to the cAMP molecule, notably the NHB and the C-terminal hinge/lid region (Fig. 2*B*). Both regions are predicted to undergo conformational changes upon ligand binding (13). The NMR data confirm that initial binding of cAMP is translated into more distal effects that lead to the activation of the protein.

An Active Epac Population in the Absence of cAMP—In the ligand-free state, a second conformation was assigned for several residues (Figs. 1*B* and 2C). The second conformation has chemical shift values of its cAMP-bound-state counterparts, suggesting the presence of a static population of >20% of the active conformation as estimated from peak intensities (Fig. 2*C*). Most of these residues are clustered in the NHB. The observed second conformation confirms the hypothesis that Epac exists in a dynamic equilibrium between the inactive and active states, even in the absence of cAMP (21, 22).

Proton-Deuterium Exchange—To assess the effects of cAMP binding on the stability and hydrogen bonding of Epac, proton-deuterium exchange was monitored by recording [^{15}N,^{1}H]HSQC spectra. A protein in solution samples several conformations, some of which allow backbone amide groups to undergo solvent exchange. A low exchange rate reflects strong hydrogen bonding of the corresponding residue. Residues undergoing slow exchange are found in the NHB and the central β-core, demonstrating that these parts of the protein act as stable units (Fig. 3*A*). Addition of cAMP results in only minor changes. However, increases in the protection of residues in the binding pocket are seen, for example Arg^{279}, which is directly involved in binding to cAMP as evidenced by the crystallographic data from PKA (6, 7) and ion channel (11, 12). Interest-

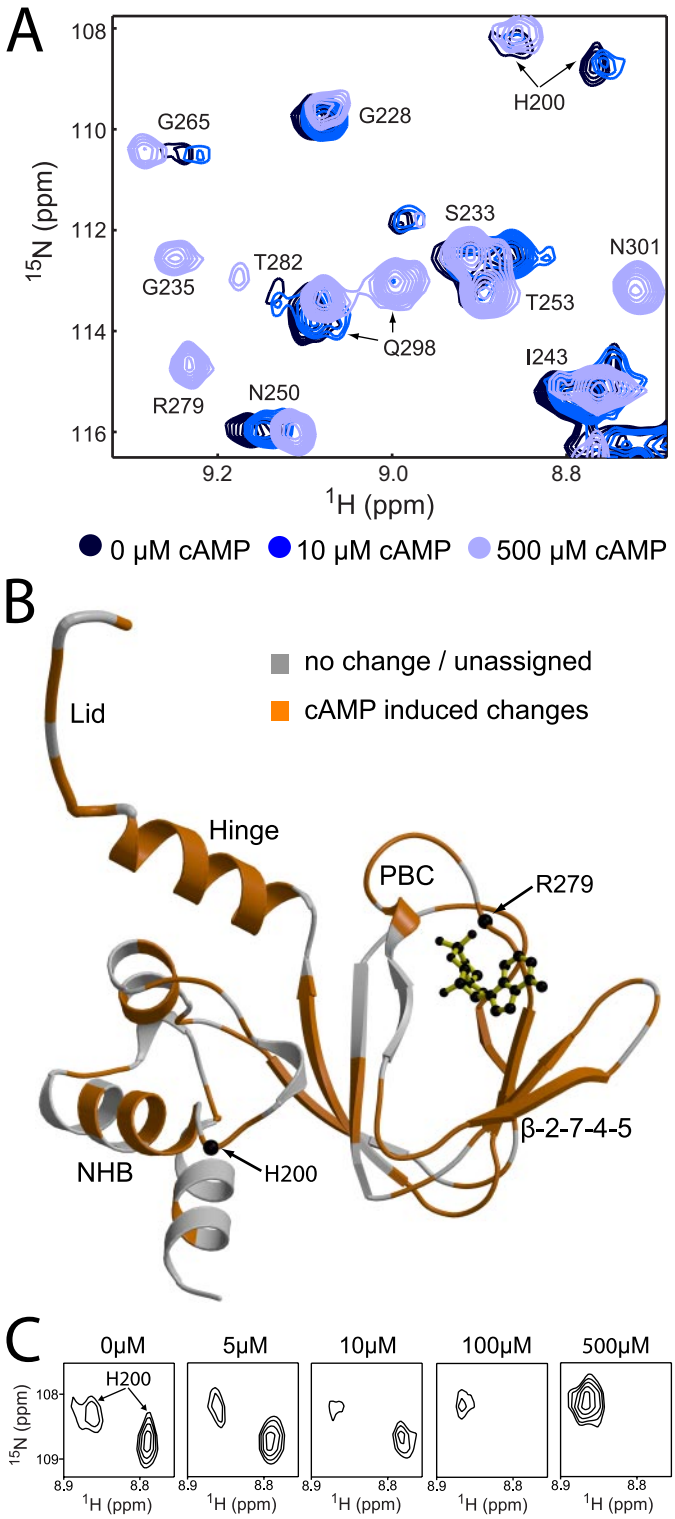

FIGURE 2. **cAMP-induced changes.** *A*, overlay of [^{15}N,^{1}H]HSQC spectra recorded in the presence of 0, 10, and 500 μM cAMP. The chosen section is representative for the quality of the obtained spectra and shows the kinds of exchange behavior observed during the titration. *B*, the residues affected by cAMP were mapped on the second CNB domain of Epac2 taken from the crystal structure of the autoinhibited Epac2 (Protein Data Bank code 2bvy) (10). The cAMP molecule shown in *ball-and-stick* representation was placed according to the cAMP-bound structure of PKA (Protein Data Bank code 1rgs) (6). *C*, for several residues, two alternative conformations were assigned in the absence of cAMP. One of these conformations corresponds to the cAMP-bound chemical shift. One example, residue His^{200} is shown during the course of titration.

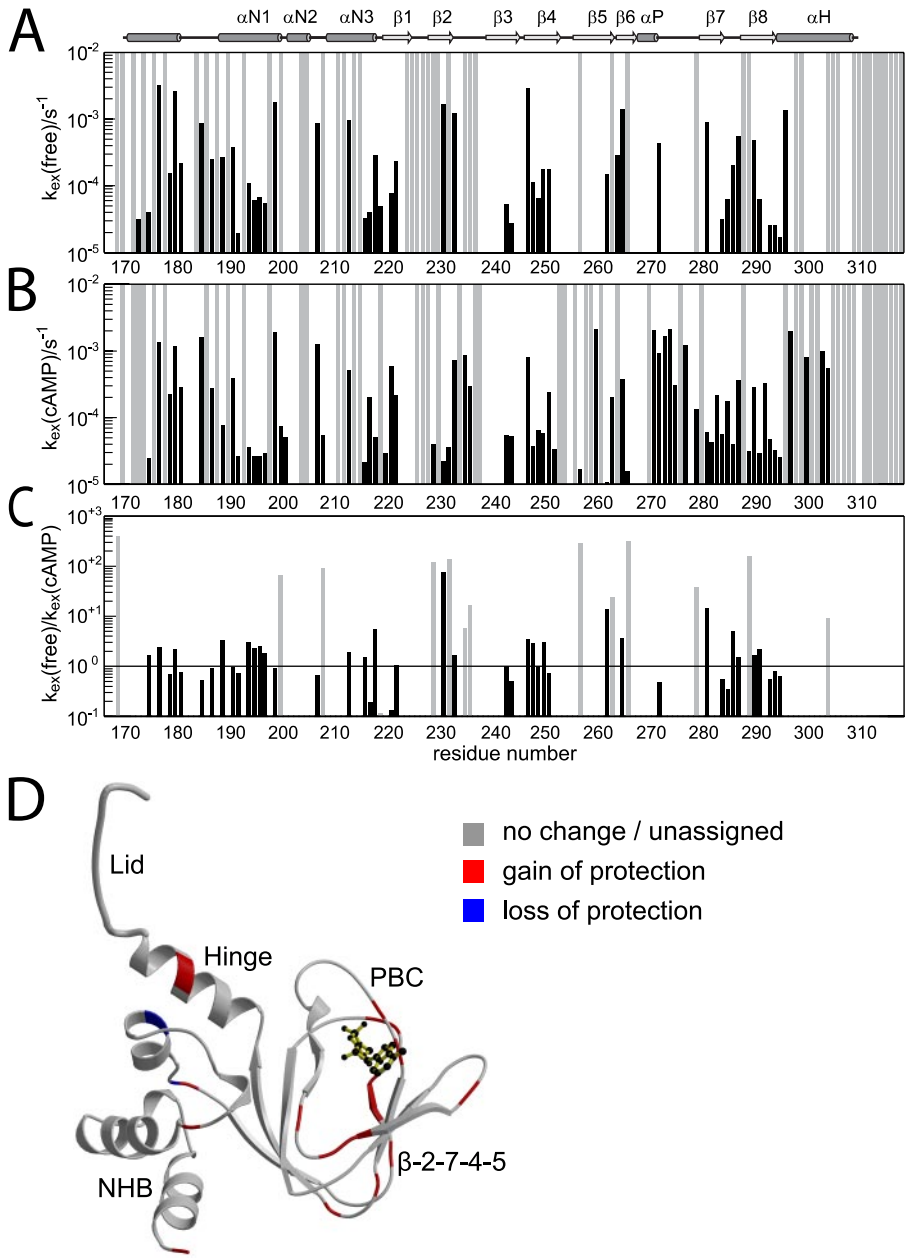

FIGURE 3. **Deuterium exchange in the presence and absence of cAMP.** The exchange rate of the individual residues in the absence (*A*) and presence (*B*) of cAMP were plotted against the residue number. *Gray bars* represent residues for which the exchange reaction was completed within 900 s, the dead time of the experiment. Residues without a bar are either a proline or unassigned. *C*, the ratio of the exchange rates in the absence and presence of cAMP is plotted against the residue number. A value bigger than one indicates gain of protection and a value smaller than one indicates loss of protection in the presence of cAMP. *Gray bars* represent residues for which the exchange reaction either in the absence or the presence of cAMP was completed within the dead time of the experiment (900 s). To calculate the ratio, a k_{ex} of 0.005 s^{-1} was assumed for residues that underwent complete exchange within the dead time, so that the calculated ratio in these cases is underestimated. *D*, residues with an at least 4-fold gain or loss in protection were mapped onto the CNB domain of Epac2 in *red* and *blue*, respectively.

ingly, residues outside the core binding pocket are also affected. Ile^{304} in the hinge helix gains protection, and Ala^{217}, Leu^{219}, and Phe^{221} in the loop connecting the NHB and β1 lose protection (Fig. 3, *B–D*). This demonstrates again that cAMP induces conformational changes in the NHB and the hinge helix and that the cAMP-bound state is a dynamic conformation.

Effects of cAMP Antagonists—Rp-cAMPS and N^6-phenyl-cAMP (Fig. 4*A*) are competitive inhibitors of Epac that bind to Epac with similar affinity as cAMP but are unable to efficiently activate the protein (23). These analogues were used to separate effects attributed solely to binding of the ligand from those attributed to conformational changes resulting in activation.

Rp-cAMPS, where the equatorial phosphate oxygen of the phosphate that interacts with the PBC is replaced by a sulfur, was titrated into the CNB domain, and changes in the [^{15}N,^{1}H]HSQC spectra were mapped onto the domain structure (Fig. 4*A*). As with cAMP, most residues in the β-2-7-4-5 sheet are affected by the presence of Rp-cAMPS. Furthermore, the chemical shifts of these residues are comparable with the cAMP-bound shifts, indicating that Rp-cAMPS occupies the same or a very similar position in the binding pocket (for example, Thr^{261} in Fig. 4*B*). However, unlike cAMP, the PBC is barely affected by the presence of Rp-cAMPS. Similarly, fewer changes are observed for residues situated in the NHB or the hinge helix (for example Glu^{196} in Fig. 4*B*). The limited changes that are observed for the hinge helix are different from those induced by cAMP, as indicated by the different chemical shifts of the peaks (for example, Ile^{303} in Fig. 4*B*). Thus, the precise engagement of the PBC is a prerequisite for conformational changes in the hinge and the NHB.

To further study the activation mechanism, the antagonist N^6-phenyl-cAMP was used. With this analogue, the base is modified at the 6 position by the extension of a phenyl group, and therefore its structural effects on Epac should be distinct from Rp-cAMPS. N^6-phenyl-cAMP induces changes in the β-2-7-4-5 sheet similar to those induced by cAMP and Rp-cAMPS, indicating the proper positioning of N^6-phenyl-cAMP in the binding pocket (Fig. 4*A*; for example, Thr^{261} in Fig. 4*B*). However, unlike Rp-cAMPS, N^6-phenyl-cAMP does affect residues of the PBC, initiating the first step in the activation process. Subsequently, much more extensive changes are observed in the NHB and hinge region than with Rp-cAMPS (for example, Thr^{187} in Fig. 4*B*). However, these changes are often different from those caused by cAMP, as evi-

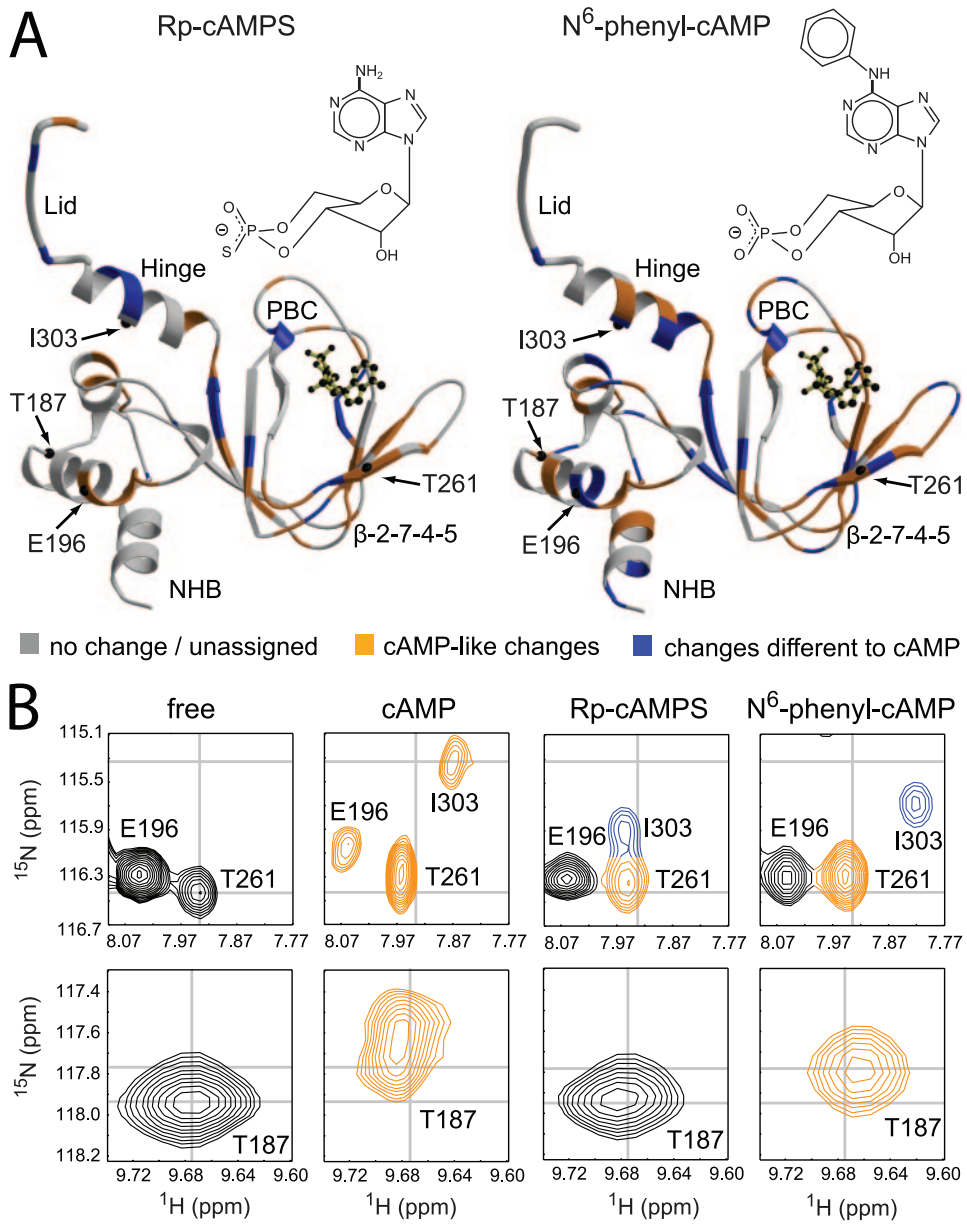

FIGURE 4. **Effects of competitive inhibitors.** *A*, the chemical structures of Rp-cAMPS and N^6-phenyl-cAMP are shown. Residues that undergo chemical shift changes upon titration with Rp-cAMPS and N^6-phenyl-cAMP were mapped onto the structure of Epac2 (see Fig. 2). Residues with the same chemical shift changes as observed during the titration with cAMP are highlighted in *orange* and residues with different chemical shift changes in *blue*. *B*, the peaks for Glu^{196}, Thr^{261}, Ile^{303}, and Thr^{187} are shown in the absence of ligand and the presence of cAMP, Rp-cAMPS, and N^6-phenyl-cAMP and their chemical shifts compared. Glu^{196} and Thr^{187} are localized in the NHB, Thr^{261} in the β-2-7-4-5 sheet, and Ile^{303} in the hinge.

denced by their different chemical shifts (for example, Ile^{303} in Fig. 4*B*). Thus, while the PBC adopts an active conformation and releases the steric restraint that prevents the movement of the hinge, the final active conformation is not properly stabilized due to the inability of N^6-phenyl-cAMP to properly interact with the lid.

Superactivation of Epac—To further explore ligand-induced activation of Epac, we studied 8-pCPT-2′-O-Me-cAMP, which induces higher activity than cAMP and hence acts as a superactivator of the protein (23–25). Mapping 8-pCPT-2′-O-Me-cAMP-induced changes from the [^{15}N,^{1}H]HSQC spectra onto the Epac structure, it is clear that this compound affects similar regions of the CNB domain as cAMP, illustrating the common activated conformation produced by the two molecules (Fig. 5, *A* and *B*). However, the type of chemical exchange seen is quite different. These differences are particularly obvious for the hinge helix and the lid, as well as for parts of the PBC (Fig. 5*B*). Peaks that undergo slow exchange in the course of the titration with cAMP fail to appear during the titration with 8-pCPT-2′-O-Me-cAMP (Fig. 5, *A* and *B*). These peaks are now in a conformational exchange whose time scale is undetectable in this NMR experiment, indicating that 8-pCPT-2′-O-Me-cAMP differently affects the protein dynamics in this region. Therefore, while the previous inhibitors highlighted the role of proper structural rearrangements in activation, the superactivator, which induces a similar conformation as cAMP, suggests that dynamics also play a role in protein activation.

DISCUSSION

In this study we analyzed the structural consequence of cAMP binding to the CNB domain of Epac and addressed the mechanism of antagonism as well as superactivation mediated by cAMP analogues. We demonstrated the successive nature of the agonist-induced conformational changes, experimentally validating a universal model by which CNB domains sense cAMP and translate the initial binding event to changes in the outer parts of the domain.

Interestingly, in the absence of cAMP, a double conformation was assigned to several residues, some of which correspond to the active conformation. Indeed, previous biochemical studies suggested that Epac exists in equilibrium between an inactive and active conformation, whereby binding of cAMP shifts this equilibrium to the active state (22). Based on the NMR peak intensity, the active conformation was estimated to be ~20% of the molecules. This is more than suggested by the analysis of the activity of the full-length Epac protein. However, in the full-length protein the inactive conformation of the CNB domain is stabilized by interactions of the NHB with the catalytic region (10). This restraint is missing in the isolated domain, making the inactive conformation less favored. This might also explain why the active conformation is

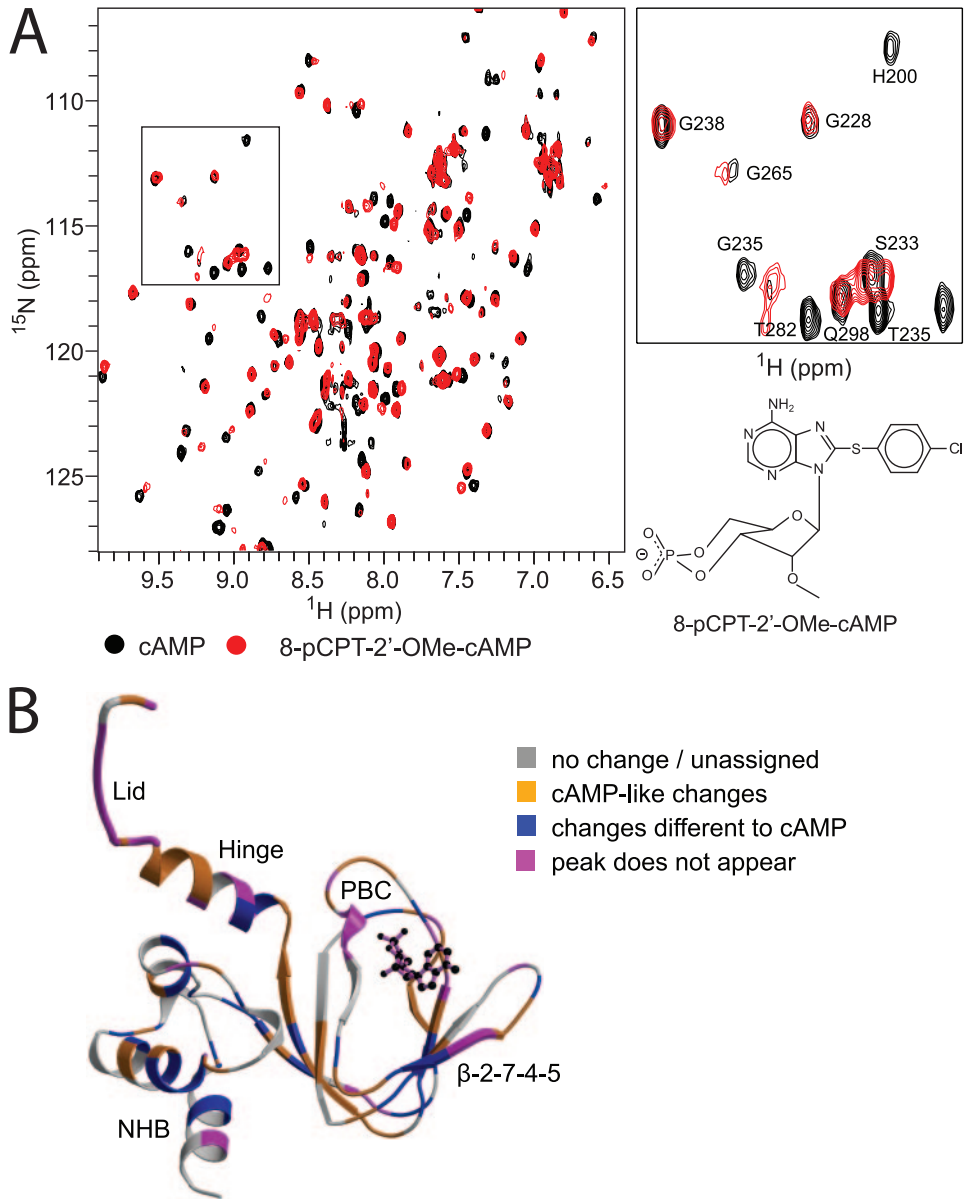

FIGURE 5. **Effects of 8-pCPT-2′-O-Me-cAMP.** *A*, overlay of [^{15}N-^{1}H]HSQC spectra recorded in the presence of cAMP (*black*) or 8-pCPT-2′-O-Me-cAMP (*red*), with a magnification of a section indicated by the *box*. The chemical structure of 8-pCPT-2′-O-Me-cAMP is shown next to the spectra. *B*, changes in residues upon titration with 8-pCPT-2′-O-Me-cAMP were mapped on the structure of Epac2 (see Fig. 2). Residues for which corresponding peaks disappear during the titration are shown in *magenta*.

fully populated in the cAMP-bound NMR spectra, even though biochemical studies suggest that this is not the case for the full-length protein. Indeed, activation of Epac requires the disruption of the interaction between the NHB and the catalytic region. The observed changes in the NHB might reflect a conformation that disfavors the interaction with the catalytic region.

Although the static structure of the active and inactive conformations is well defined by comprehensive crystallographic studies, a successive mechanism of transition was only suggested (13). According to this model, the first result of cAMP binding is a tightening of the PBC caused by its interaction with the phosphate sugar moiety of the cyclic nucleotide. As a consequence, the steric restraint is released that allows the hinge helix to move closer to the β-core, bringing the lid in close proximity to the base of cAMP and inducing a rearrangement in the NHB. This allows the lid to interact with the base and thereby to stabilize the active conformation. Using the antagonists Rp-cAMPS and N^6-phenyl-cAMP, we trapped the CNB domain in different steps of the activation process, confirming its successive nature experimentally. With Rp-cAMPS, the ability to productively interact with the PBC is impaired. Consequently, fewer changes were observed in the PBC than with cAMP and the NHB and the C-terminal hinge/lid region remained largely unaffected. N^6-phenyl-cAMP, which is presumably unable to properly interact with the lid, does engage the PBC. Subsequently, changes in the NHB and the C-terminal region are observed. These changes differ from those induced by cAMP, reflecting the principle freedom of the hinge helix to move. However, this movement remains random because the lid cannot be trapped by the interaction with the base. These data clearly demonstrate that the tightening of the PBC alone is not sufficient for activation and that an additional, precise, interaction of the lid and the base is required to establish the full active state.

Finally, we observe that although the superactivator 8-pCPT-2′-O-Me-cAMP causes similar conformational changes as cAMP, it affects the intrinsic dynamics of the CNB domain differently by inducing chemical shift changes on a different time scale than cAMP. This causes peaks that undergo slow exchange upon titration with cAMP to disappear from the spectrum with the superactivator. This highlights the added role of dynamics in activation, in addition to the structural rearrangements required to place the protein in the proper active conformation.

The first CNB domain of PKA was recently analyzed in a similar NMR-based approach (26–28). As observed for Epac, cAMP binding induces large chemical shift changes in the PBC and in the outer helical segments of the domain (26). In PKA an additional region is affected by cAMP binding, the β2–β3 loop with Asp^{170} (26, 27, 29). Even though Asp^{170} is not directly involved in the interaction with the kinase domain (8), mutation of this residue to alanine results in a protein that has a higher affinity for the kinase domain in the cAMP-bound state (30). Asp^{170} of PKA corresponds to Thr^{239} of Epac, which

remained unassigned. To date, there is no experimental evidence that Thr^{239} is required for the activation of Epac. Thus, while Epac and PKA bind cAMP in a common manner, they communicate to their respective catalytic regions in a way that is adapted to the requirements of the specific protein. This is further demonstrated by differences in protein stability in the regions that contact the catalytic domain. Whereas the NHB of Epac remains protected from hydrogen-deuterium exchange even in the absence of ligand, the NHB of PKA undergoes rapid exchange in either state. Finally, PKA and Epac are characterized by different cAMP analogue selectivity. 8-pCPT-2′-O-Me-cAMP acts as a superactivator of Epac but is unable to bind and activate PKA, whereas N^6-phenyl-cAMP activates PKA but acts as an antagonist on Epac (24, 25). Understanding the mechanistic consequences of these differences will help in the design of new selective activators and inhibitors for the individual cAMP pathways.

Acknowledgments—We thank Dorothee Kuehlmann for cloning the Epac1 CNB domain fragment and Peter Bayer, Hans Robert Kalbitzer, Atsushi Shimada, and Alfred Wittinghofer for contributions in the initial phase of the project.

REFERENCES

1. Beavo, J. A., and Brunton, L. L. (2002) *Nat. Rev. Mol. Cell. Biol.* **3,** 710–718
2. Shabb, J. B., and Corbin, J. D. (1992) *J. Biol. Chem.* **267,** 5723–5726
3. Bos, J. L. (2003) *Nat. Rev. Mol. Cell. Biol.* **4,** 733–738
4. Seino, S., and Shibasaki, T. (2005) *Physiol. Rev.* **85,** 1303–1342
5. Bos, J. L. (2006) *Trends Biochem. Sci.* **31,** 680–686
6. Su, Y., Dostmann, W. R., Herberg, F. W., Durick, K., Xuong, N. H., Ten Eyck, L., Taylor, S. S., and Varughese, K. I. (1995) *Science* **269,** 807–813
7. Diller, T. C., Madhusudan, Xuong, N. H., and Taylor, S. S. (2001) *Structure (Camb.)* **9,** 73–82
8. Kim, C., Xuong, N. H., and Taylor, S. S. (2005) *Science* **307,** 690–696
9. Rehmann, H., Prakash, B., Wolf, E., Rueppel, A., de Rooij, J., Bos, J. L., and Wittinghofer, A. (2003) *Nat. Struct. Biol.* **10,** 26–32
10. Rehmann, H., Das, J., Knipscheer, P., Wittinghofer, A., and Bos, J. L. (2006) *Nature* **439,** 625–628
11. Zagotta, W. N., Olivier, N. B., Black, K. D., Young, E. C., Olson, R., and Gouaux, E. (2003) *Nature* **425,** 200–205
12. Clayton, G. M., Silverman, W. R., Heginbotham, L., and Morais-Cabral, J. H. (2004) *Cell* **119,** 615–627
13. Rehmann, H., Wittinghofer, A., and Bos, J. L. (2007) *Nat. Rev. Mol. Cell. Biol.* **8,** 63–73
14. Canaves, J. M., and Taylor, S. S. (2002) *J. Mol. Evol.* **54,** 17–19
15. Wishart, D. S., Bigam, C. G., Yao, J., Abildgaard, F., Dyson, H. J., Oldfield, E., Markley, J. L., and Sykes, B. D. (1995) *J. Biomol. NMR* **6,** 135–140
16. Delaglio, F., Grzesiek, S., Vuister, G. W., Zhu, G., Pfeifer, J., and Bax, A. (1995) *J. Biomol. NMR* **6,** 277–293
17. Cavanagh, J., Fairbrother, W. J., Palmer, A. G., and Skelton, N. J. (2007) *Protein NMR Spectroscopy, Principles and Practice,* 2nd Ed., Academic Press, San Diego, CA
18. Cornilescu, G., Delaglio, F., and Bax, A. (1999) *J. Biomol. NMR* **13,** 289–302
19. Yu, S., Fan, F., Flores, S. C., Mei, F., and Cheng, X. (2006) *Biochemistry* **45,** 15318–15326
20. Brock, M., Fan, F., Mei, F. C., Li, S., Gessner, C., Woods, V. L., Jr., and Cheng, X. (2007) *J. Biol. Chem.* **282,** 32256–32263
21. Rehmann, H., Rueppel, A., Bos, J. L., and Wittinghofer, A. (2003) *J. Biol. Chem.* **278,** 23508–23514
22. Rehmann, H. (2006) *Methods Enzymol.* **407,** 159–173
23. Rehmann, H., Schwede, F., Doskeland, S. O., Wittinghofer, A., and Bos, J. L. (2003) *J. Biol. Chem.* **278,** 38548–38556
24. Enserink, J. M., Christensen, A. E., de Rooij, J., van Triest, M., Schwede, F., Genieser, H. G., Doskeland, S. O., Blank, J. L., and Bos, J. L. (2002) *Nat. Cell Biol.* **4,** 901–906
25. Christensen, A. E., Selheim, F., de Rooij, J., Dremier, S., Schwede, F., Dao, K. K., Martinez, A., Maenhaut, C., Bos, J. L., Genieser, H. G., and Doskeland, S. O. (2003) *J. Biol. Chem.* **278,** 35394–35402
26. Das, R., Abu-Abed, M., and Melacini, G. (2006) *J. Am. Chem. Soc.* **128,** 8406–8407
27. Das, R., Esposito, V., Abu-Abed, M., Anand, G. S., Taylor, S. S., and Melacini, G. (2007) *Proc. Natl. Acad. Sci. U. S. A.* **104,** 93–98
28. Das, R., and Melacini, G. (2007) *J. Biol. Chem.* **282,** 581–593
29. Abu-Abed, M., Das, R., Wang, L., and Melacini, G. (2007) *Proteins* **69,** 112–124
30. Gibson, R. M., Ji-Buechler, Y., and Taylor, S. S. (1997) *J. Biol. Chem.* **272,** 16343–16350